J. Physiol. (1987), **391**, *pp.* 631–649
With 12 text-figures
Printed in Great Britain

SODIUM AND POTASSIUM CURRENTS IN ACUTELY DEMYELINATED INTERNODES OF RABBIT SCIATIC NERVES

BY S. Y. CHIU AND W. SCHWARZ*

From the University of Wisconsin, Department of Neurophysiology, 283 Medical Sciences Building, 1300 University Avenue, Madison, WI 53706, U.S.A.

(*Received 28 October 1986*)

SUMMARY

1. Voltage-clamp experiments were performed on single internodes isolated from rabbit sciatic nerve fibres acutely demyelinated with the detergent lysolecithin or a synthetic analogue, lysophosphatidyl choline palmitoyl.

2. The extent of demyelination was monitored by a gradual increase in the internodal leak conductance and capacitance. Voltage- and time-dependent inward and outward currents, absent during the early phase (30–40 min) of detergent treatment, appeared during the final phase (40–60 min) of treatment.

3. The internodal ionic currents elicited by depolarizations consisted of three components pharmacologically identified as (a) a transient sodium current which was inhibited by tetrodotoxin, (b) a delayed rectifying potassium current which was inhibited by internal caesium and (c) a time-dependent current that was abolished by replacement of external chloride with ascorbate.

4. The current–voltage relations and h_∞ curves for the internodal sodium current were similar in shapes to those of the nodal sodium current.

5. The amplitudes of the three internodal currents increased with the increase in the measured internodal capacity during the final phase of demyelination.

6. At high degrees of demyelination a peak sodium current of about 90 nA could be observed in an internodal segment of 100 μm length.

7. Interestingly, the membrane capacity measured at the time of such a large sodium current was about 10 times larger than could be accounted for by the axonal membrane in the recording pool alone. A suggestion is made that this represents lysolecithin-induced membrane fusion between the Schwann cell and the internodal axon.

INTRODUCTION

Recent studies have shown that myelination affects the distribution of ion channels along an axon (for review, see Waxman & Ritchie, 1985). The presence of ion channels in the internode of a myelinated fibre was directly demonstrated in voltage-clamp studies using single isolated internodes. Chiu & Ritchie (1982) performed

* Permanent address: Max-Planck-Institut fur Biophysik, Heinrich-Hoffmannstr. 7, D-6000 Frankfurt/M, FRG.

voltage-clamp studies on single frog internodes after treating them with lysolecithin, an agent known to cause demyelination (Hall & Gregson, 1971). After about 45 min a large potassium current, but no sodium current, was recorded. These results have been interpreted as an uncovering of pre-existing channels on the internodal axolemma by acute myelin removal (Chiu & Ritchie, 1982). Recently, Grissmer (1986) found that in the frog, a small internodal sodium current could in fact be detected if the large potassium current was blocked.

In this study, a similar voltage-clamp analysis has been made of the internodal currents in rabbit internodes after treatment with lysolecithin or a synthetic analogue, lysophosphatidyl choline palmitoyl. The results show that not only could a large potassium current be detected, but in addition, a significant internodal sodium current, much larger than that in frog, was also detected. These currents could account for continuous conduction in demyelinated mammalian nerve fibres as proposed by Bostock & Sears (1978), and raises the issue of whether the axonal membrane covered by the myelin sheath in mammalian nerves is inherently excitable. Interestingly the internodal membrane capacity recorded at times when sodium currents appeared maximal was about 10 times too large to be accounted for by axonal membranes alone. Since lysolecithin is known to induce fusion of biological membranes (Poole, Howell & Lucy, 1970), a suggestion is made that membrane fusion might have occurred between the Schwann cell and the axon. In view of recent patch-clamp studies showing that neuronal-like sodium channels are present in Schwann cells from both newborn (Chiu, Shrager & Ritchie, 1984; Shrager, Chiu & Ritchie, 1985) and adult rabbits (Chiu, 1987), the possibility is discussed whether the internodal axon normally possesses these channels, or whether it acquires them through membrane fusion with the Schwann cells. A preliminary account of this work has appeared elsewhere (Chiu & Schwarz, 1987).

METHODS

Voltage-clamp studies were performed with the method of Nonner (1969). Adult rabbits, 14–20 weeks old, were killed with a sharp blow to the back of the neck. The sciatic nerves were taken out and desheathed as described previously (Chiu, Ritchie, Rogart & Stagg, 1979). Large single myelinated fibres (18–20 μm in diameter) were isolated from the nerve trunk, with two nodes of Ranvier visible under the dissection microscope. A single fibre was then mounted in the nerve chamber as shown in the schematic drawing in Fig. 1. The entire internode spanned the four pools, with the nodes located in the two end pools (C and E). The recording pool (A) contained 100 μm length of internode; this internodal segment was demyelinated by applying a Locke solution containing either lysolecithin (0·2%) or lysophosphatidyl choline palmitoyl (0·1%, Sigma) as detergent. The node in pool E was located just next to the partition between pools A and E. The distance measured from the centre of pool A to the node in pool E was about 150–250 μm (see Fig. 1). In most experiments, the fibre was cut in the end pools leaving two intact nodes in pools C and E. In a few experiments, the node in pool E was also cut. All experiments were done at a room temperature of about 20 °C.

Protocol of measurement

The pulse protocols were essentially similar to those used in previous demyelination studies on frog internodes (Chiu & Ritchie, 1982). Briefly, under voltage-clamp, a hyperpolarizing pulse of amplitude −45 mV was applied repeatedly from the holding potential to monitor leakage and capacity currents during demyelination. At various times, a family of depolarizations was applied to check for appearance of voltage-dependent currents. After 40–60 min, or when signs of non-

linear outward or inward currents appeared, pool A was washed with a detergent-free solution, and the experiments described in the Results section were performed. At the end of several experiments, the absolute value of the holding potential applied during the experiment was determined from the voltage displacement in pool A after the membrane of the internodal axon in pool A was finally destroyed by the detergent. Such measurements yielded a value of $-65{\cdot}0 \pm 3{\cdot}3$ mV ($n = 11$). All membrane potentials in this study are thus reported in absolute values, using the value of -65 mV for the absolute holding potential. For calibration of the currents, the longitudinal axoplasmic

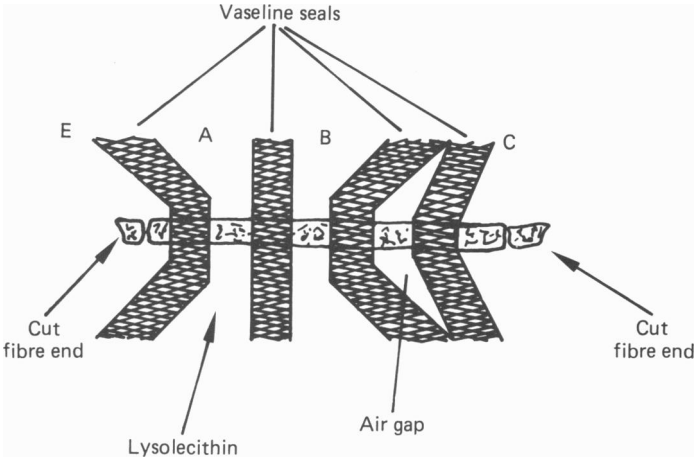

Fig. 1. Schematic drawing of the mounting of an internode for voltage-clamp studies. The nerve chamber was of the Nonner type (Nonner, 1969) A, B, C and E represent pools filled with solutions as described in the text. Pool A contains the internodal segment to be demyelinated. The width of pool A was fixed at 100 μm for all experiments. The distance from the node in pool E to the middle of pool A is about 150–250 μm. The partitions between the pools were covered with Vaseline (cross-hatched) for insulation and an additional air gap was placed between pools B and C. The arrows in pools C and E indicate where the fibre was usually cut.

resistance between pools A and E was determined from electrical measurements (Sigworth, 1980). An average value for the axoplasmic resistance of $6{\cdot}2 \pm 1{\cdot}1$ MΩ ($n = 11$) was obtained; this value was used for current calibration in experiments where such measurements had not been performed.

For determination of current–voltage relations a pre-pulse of 100 ms duration to -110 mV was followed by a series of various depolarizing test pulses. For h_∞ curves, pre-pulses to various potentials were followed by a fixed test pulse, and the changes of the inward peak currents were determined. Unless otherwise mentioned, the current records shown were corrected for linear leakage and capacitative currents using scaled currents from hyperpolarizing pulses.

As in previous studies on demyelinated frog internodes (Chiu & Ritchie, 1982; Grissmer, 1986) the capacitive current consisted of a fast and a slow component. The total membrane capacity ($C_f + C_s$) was calculated from the integral (charge) of capacity transient current during the first 10 ms, after subtraction of a steady leakage current. The initial fast capacity (C_f) was calculated by subtracting the slow capacity current component from the record by fitting a single exponential to the slow component of the capacitive current (for more details, see legend of Fig. 10 and Results). The capacity current was elicited with a hyperpolarizing pulse from the holding potential of -65 to -110 mV, and sampled at every 10 or 50 μs. Currents were filtered at 2 kHz (low pass 8-pole Bessel, Frequency Devices).

Solutions

The normal bath solution in the pool A contained (mM): NaCl, 154; KCl, 5·6; $CaCl_2$, 2·2; morpholinopropionyl sulphonate buffer (pH 7·4), 10; and 0·3% glucose. Several procedures were

used in an attempt to prolong fibre survival after demyelination. First, detergent-free Locke solutions containing bovine albumin (1%, Sigma) and 5 mM-adenosine triphosphate (ATP) were used for washing the internodal segment to halt detergent action (Grissmer, 1986). ATP has been suggested to inhibit the lytic action of lysolecithin by promoting its acylation at the plasma membrane (Webster & Alpern, 1964). Secondly, lysophosphatidyl choline palmitoyl, a synthetic analogue of lysolecithin, was used since it was found to be a more potent agent. However, no significant prolongation of fibre survival could be obtained with these procedures when compared with earlier studies in frog using lysolecithin (Chiu & Ritchie, 1982). Thus in later experiments, lysolecithin was used instead of the synthetic palmitoyl analogue, and bovine albumin and ATP were frequently omitted from the wash solution. The successful prolongation of fibre survival obtained by Grissmer (1986) may possibly be attributed to the lower temperature (15 °C) used in his experiments.

The ends of the fibres (in pools C and E) were cut either in a 150 mM-KCl or 150 mM-CsCl solution (internal solution). In some experiments, 10 mM-NaCl was added to the internal solution to yield a measurable reversal potential for sodium currents.

RESULTS

Internodal segments, each 100 μm in length, were voltage clamped and exposed to detergent. The leak and capacity currents underwent a characteristic gradual increase similar to that already described for frog internodes (Chiu & Ritchie, 1982; Grissmer, 1986). During the first 30–40 min, no voltage-dependent internodal currents could be detected. Subsequently, voltage-dependent currents appeared. The amplitudes of these currents increased rapidly, and were accompanied by a concomitant increase in the internodal membrane capacity. The time between the first appearance of voltage-dependent currents and the disruption of the internodal membrane was in the range of a few seconds to several minutes. Washing away the detergent upon first signs of internodal currents delayed the membrane breakdown in a few experiments for up to about 30 min to allow a measurement of the current–voltage relations; however, such a prolonged fibre survival was only rarely achieved.

Figure 2 shows a typical family of rabbit internodal membrane currents obtained in the presence of an internal KCl solution after exposure to detergent for about 33 min. It can clearly be seen that the currents of acutely demyelinated internodes of rabbit nerve fibres consist of an early transient inward current, and a large late outward current.

The internodal ionic current consists of three components

The transient inward current clearly resembles the sodium current seen in excitable membranes. Figure 3 shows the effect of tetrodotoxin (TTX) on the early inward current in an experiment in which the detergent action was halted by repeated wash with a detergent-free Locke solution. This wash delayed membrane breakdown for several minutes, but also prevented the full increase of the inward current from being achieved. It can be seen that the inward current (Fig. 3*A*) was completely eliminated by 1 μM-TTX (Fig. 3*B*). The time it took for complete inhibition to occur was about 5 min, suggesting a slow diffusion of the toxin through a partially destroyed myelin sheath.

The large outward current in Fig. 2 clearly resembles the internodal potassium current seen in demyelinated frog internodes. Indeed, if CsCl was used instead of KCl

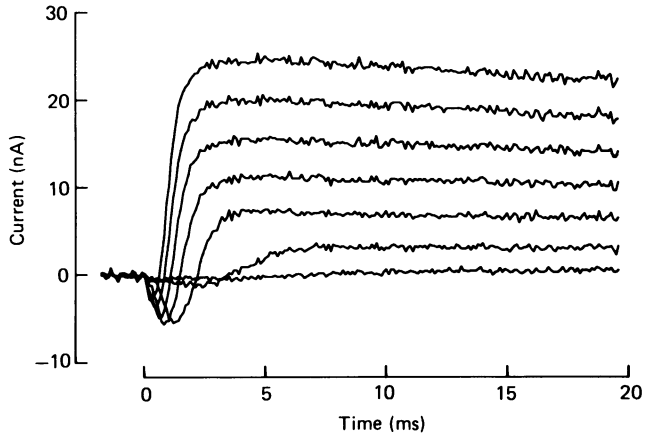

Fig. 2. Membrane currents obtained from a single rabbit internode after acute partial demyelination. The demyelinated segment was bathed in a normal Locke solution and a 150 mM-KCl solution was present in the side pools. The family of currents was generated by a series of depolarizations from −45 to +75 mV in 20 mV increments, preceded by a 100 ms pre-pulse to −110 mV. Holding potential was −65 mV between pulses. Currents recorded 32 min after treatment with lysophosphatidyl choline palmitoyl (0·1 %).

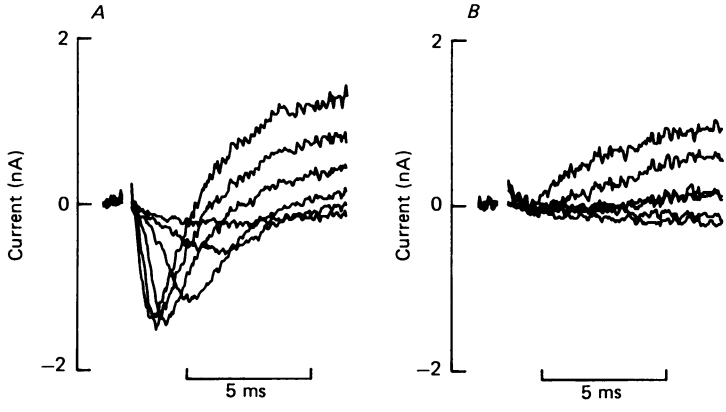

Fig. 3. Internodal membrane currents before (*A*) and after (*B*) external application of 1 μM-TTX. A CsCl solution was present internally to inhibit potassium currents. The families of currents were generated by a series of depolarizations to −65, −45, −25, +15, +55 and +95 mV, preceded by a 100 ms hyperpolarizing pre-pulse to −110 mV. Currents were recorded about 55 min after application of detergent.

as the internal solutions during demyelination, the outward current observed towards the final phase of demyelination became much reduced in amplitudes. Figure 4*A* shows an experiment in which the internal solution was a 150 mM-CsCl solution. Clearly, only a much smaller outward current was obtained (compare Fig. 2 with Fig. 4*A*) and no further increase in outward current was detected even if demyelination was allowed to proceed further to ultimate membrane breakdown. This sensitivity to caesium ions suggests that a major component of the outward

current (as in Fig. 2) is a delayed rectifying potassium current. External application of 10 mM-tetraethylammonium (TEA) had no further effects on the residual caesium-insensitive outward current in Fig. 4*A*.

The residual outward current in Fig. 4*A* could be mediated by an outward movement of positively charged caesium ions present in the axoplasm, as suggested by Grissmer (1986) for a similar residual current in demyelinated frog internodes. Another explanation would be an inward movement of negatively charged chloride

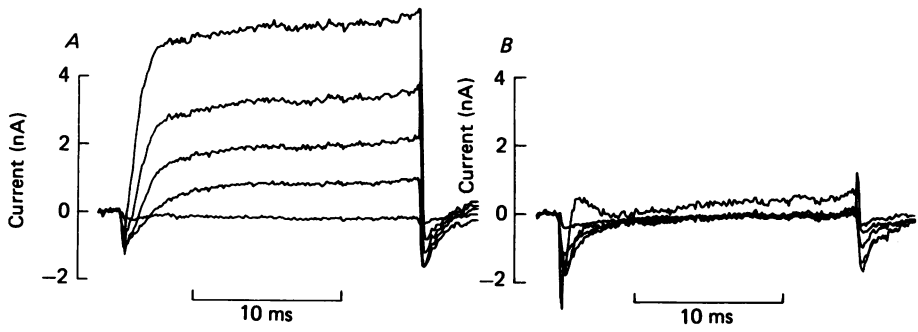

Fig. 4. Internodal membrane currents with chloride (*A*) and ascorbate (*B*) as the major external anions. Currents were from the same internodal segment. *B* was recorded 30 s after replacement of the external chloride with ascorbate. A CsCl solution was present to block potassium currents. The families of currents were generated by a series of depolarizations from −65 to +95 mV in 40 mV increments. Currents were recorded about 39 min after application of detergent.

ions present in the external solutions. The experiment in Fig. 4*B* supports the latter possibility. Here, the outward current was found to be virtually abolished upon replacing the external chloride by ascorbate, a large anion shown to be impermeable to anion-selective channels in mammalian astrocytes (Bevan, Chiu, Gray & Ritchie, 1985). This effect of ascorbate was fully and rapidly reversible upon wash, suggesting that the inhibition of the outward current was not due to membrane damage. This caesium-insensitive outward current, detected consistently in the demyelinated rabbit internodes, is thus likely to be a chloride current similar to that found in mammalian astrocytes (Bevan *et al.* 1985). Also consistent with this interpretation is that the inward tail currents seen in Fig. 4*A*, which presumably reflected an outward movement of chloride, were not affected by external ascorbate (Fig. 4*B*). No further studies were carried out on this presumed chloride current which accounts for only about 5% (see Discussion) of the total outward current.

Current–voltage and h_∞ relations

The current–voltage relations for the various components of internodal currents are shown in Fig. 5 at an early stage of demyelination (open symbols) and at a late stage of demyelination (filled symbols). Figure 5*A* shows the current–voltage relations for the peak sodium current (square symbols) and the late outward current (diamond symbols) obtained from an internodal segment demyelinated in the presence of an internal CsCl solution. The corresponding relations from a different experiment for the late outward current with KCl as the internal solution are shown

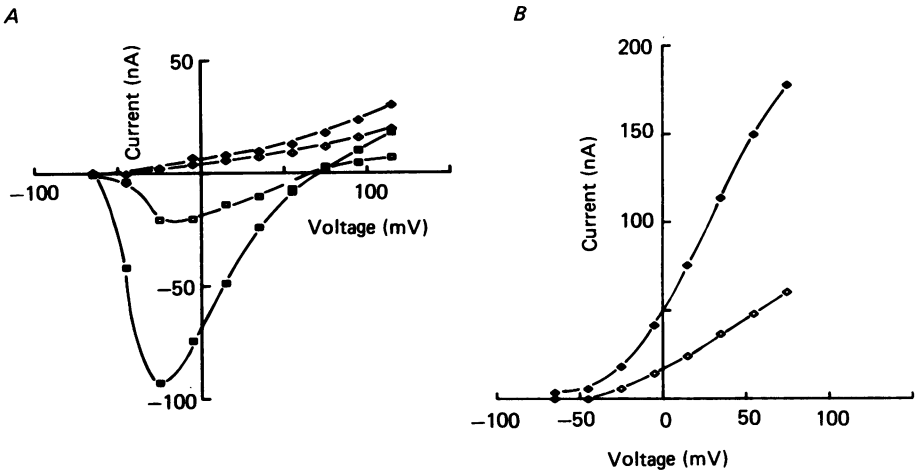

Fig. 5. Current–voltage relations of the three different components of internodal membrane currents. Open symbols refer to an early stage of demyelination, filled symbols to a stage 5 min later which was just before membrane disruption. *A*, square symbols, peak current–voltage relations for the transient inward current; diamond symbols, caesium-insensitive outward current with 150 mM-CsCl plus 10 mM-NaCl as internal solution. *B*, diamond symbols, late outward current with 150 mM-KCl as the internal medium.

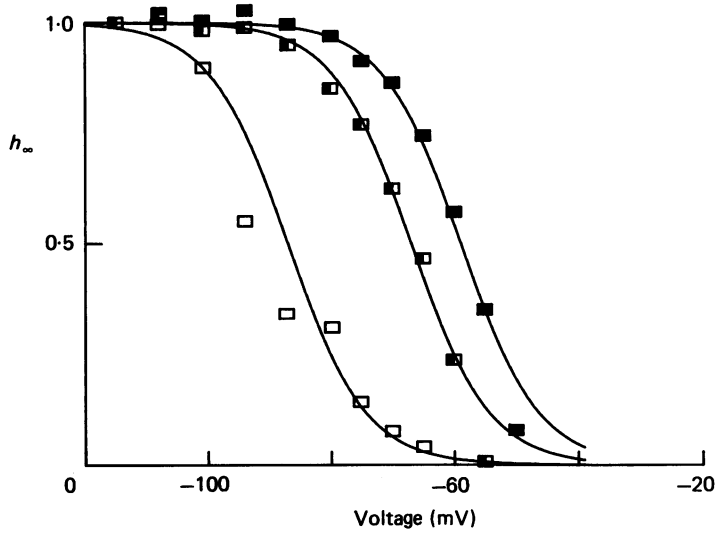

Fig. 6. h_∞ curves for the peak inward current at different times during demyelination. The different curves were obtained from the same demyelinated segment at a late stage when the inward current appeared. The speed of demyelination was then slowed down by washing with a detergent-free solution, and the h_∞ curves measured at 2 min (open symbols), 3 min (half-filled symbols) and 4 min (filled symbols) after the wash. The continuous lines were calculated from $h_\infty = 1/(1+\exp((E-E_h)/k_h))$ with $E_h = -87$ mV (open symbols), $E_h = -67$ mV (half-filled symbols) and $E_h = -59$ mV (filled symbols) and with $k_h = 6{\cdot}3$ mV in all cases. A CsCl solution was present internally to block potassium currents.

in Fig. 5*B*. Current amplitudes of all currents were found to increase as demyelination proceeds.

As can be seen in Fig. 5*A*, the peak current–voltage relations for the rabbit internodal sodium current (square symbols) clearly exhibited the characteristics of those found for sodium currents in rabbit nodes (Chiu *et al.* 1979). Furthermore, the normalized relations for the steady-state inactivation of the internodal sodium current (h_∞), as shown in Fig. 6, also resemble those of nodal membranes (Chiu *et al.* 1979). An empirical equation of the same form as that used for the rabbit node was therefore fitted to the data points (continuous lines in Fig. 6, see legend for the equation used). Interestingly the h_∞ curves for the internodal sodium currents were found to be shifted by several tens of millivolts to the depolarizing direction as demyelination proceeded. In the experiment of Fig. 6, the values for E_h (the potential for half-maximal inactivation) occurred at −87 mV (open symbols) early on during demyelination, but shifted progressively to −67 mV (half-filled symbols) and to −59 mV (filled symbols) as demyelination proceeded. The value for k_h (a measure of the steepness of the curve) is 6·3 mV for rabbit internode, which can be compared with the value of k_h = 5·7 mV for rabbit nodal sodium current (Fig. 7 of Chiu *et al.* 1979) and k_h = 8·56 mV for frog internodal sodium current (Grissmer, 1986).

Capacity versus internodal ionic currents

An indication for the progress of demyelination is the gradual increase of capacity that can be determined from the capacitive current component during a hyperpolarizing pulse. Figure 7 demonstrates in the same experiment that such a development of increasing leak and capacitance with time of experiment (shown by the superimposed current traces in *B*) is paralleled by an increase in the transient inward current and the caesium-insensitive outward current (shown by the superimposed currents obtained with a fixed depolarization to +15 mV in *A*). A similar observation was also made for the outward current in the presence of internal potassium.

A particularly interesting observation in this study is that the internodal sodium current as measured from a 100 μm internodal segment, though typically small, could achieve an extremely large amplitude during detergent treatment in some experiments. This is shown in the experiments of Fig. 8. Original internodal currents from two different experiments, *A* and *B*, are shown and a CsCl solution was present internally to block potassium currents (note the different current scales). *B* represents a typical experiment: the internodal currents, obtained shortly before membrane breakdown, showed a small sodium current which was barely seen in the original records but was revealed more clearly after leak subtraction (*D*). Typically, membrane breakdown occurred before complete demyelination could develop, preventing the full maximal internodal sodium current from being detected. The experiment of *A*, however, shows a rare case in which a significant degree of demyelination, as seen in the large surge of the initial capacity transient current, was achieved before membrane breakdown occurred. The internodal sodium current became correspondingly so large that it could easily be detected without leak subtraction (*A*) even though the voltage clamp is obviously poor under these conditions. The capacity gained a value of about 600 pF and the internodal sodium current reached a peak value of about 90 nA (*C*) before the membrane finally broke down. The peak

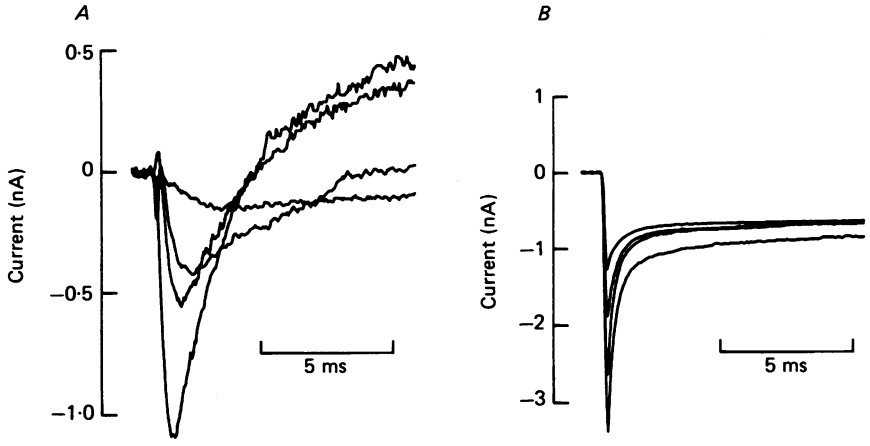

Fig. 7. Increase of internodal membrane currents with capacity during demyelination. Potassium currents in this experiment were blocked with internal CsCl and only the transient inward current and a small outward caesium-insensitive current could be seen. *A* shows superimposed leak-subtracted current records generated by a single test depolarization to +15 mV at 0·2, 5, 7·5 and 8·2 min after inward currents first appeared. Both the peak inward current and the late outward current increased with time. *B* shows the corresponding increase in capacity currents obtained with a single hyperpolarizing pulse to −110 mV.

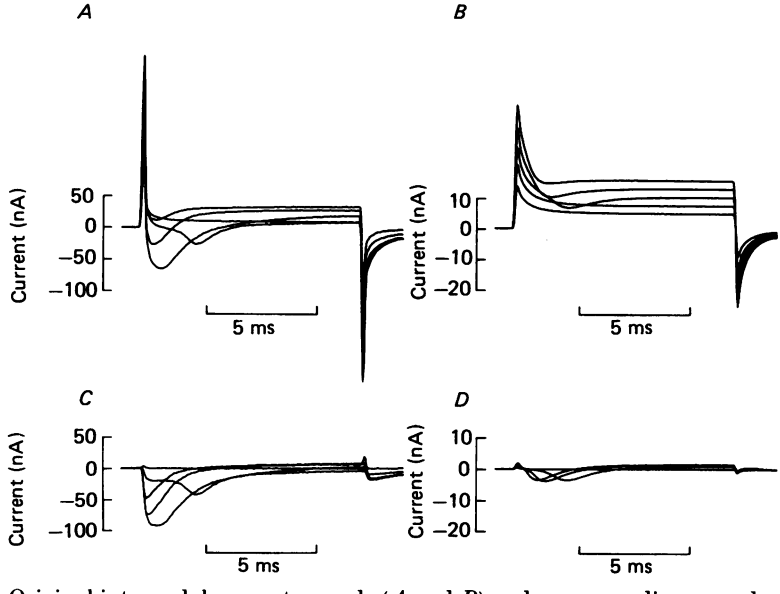

Fig. 8. Original internodal current records (*A* and *B*) and corresponding records obtained after subtraction of leak and capacity currents (*C* and *D*) from two different experiments. Currents in *A* and *C* were obtained from a demyelinated internodal segment 14 min after wash with detergent-free solution; *B* and *D* from another experiment 2 min after wash with detergent-free solution. All families of currents were generated by depolarizations from −65 to +15 mV in 20 mV steps.

current–voltage relation for the internodal sodium current from this experiment (*C*) is plotted in Fig. 5*A* (filled square symbols).

The heterogeneity in the demyelination treatment and the non-specific lytic action of the detergent on membranes made it difficult to achieve consistently the optimal condition of revealing the maximal possible sodium current. Hence, in most of the experiments, the observed peak sodium internodal sodium current was probably grossly below the maximal level that could be revealed.

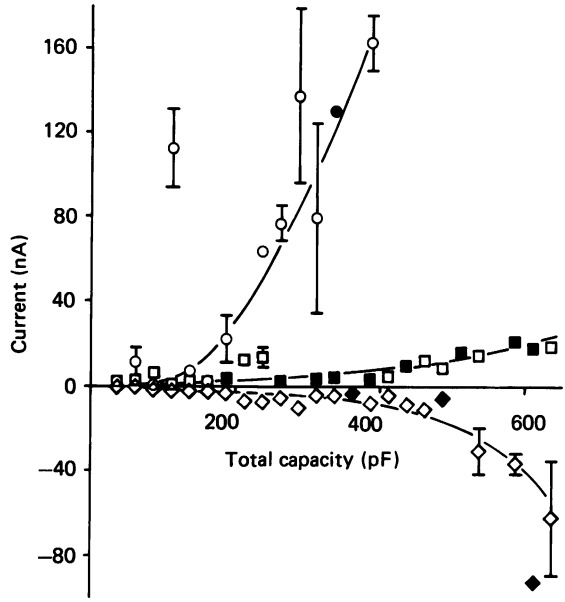

Fig. 9. Amplitudes of the different internodal currents *versus* total capacity during demyelination. Inward currents are displayed negatively and outward currents are displayed positively. Inward sodium current (diamond symbols); outward current with internal KCl (round symbols) and internal CsCl (square symbols). This amplitude for the inward current represents the peak inward sodium current measured during a sequence of depolarizations. Outward currents were measured at the end of a 10 ms depolarization to +75 mV. Data are pooled into intervals of 25 pF. Open symbols are average values from two to nineteen values of twenty-one experiments. Filled symbols are single values. Bars indicate ± S.E. of mean; if no bars are drawn the error is within the size of the symbols.

Fig. 9 summarizes results from different experiments by plotting the total capacity ((C_f+C_s), see Methods) achieved during demyelination against the corresponding various internodal ionic currents. It demonstrates that the amplitudes of the ionic currents increased with capacity, and that such a pattern was characteristic of all internodes studied.

Comparison with frog internodal sodium current density

Grissmer (1986) recently reported that sodium currents could be detected from acutely demyelinated internodes in frog. An issue of interest is the relative density of the internodal sodium currents in the two species. The plot of sodium current *versus* capacity in Fig. 9 does not allow a direct comparison with Grissmer's results

since the results have been analysed differently; here, the total capacity ($C_f + C_s$, see Methods) was used while in frog, only C_f was used (Grissmer, 1986). Thus, in order to compare internodal sodium currents between the two species, the rabbit internodal sodium currents were plotted against only C_f. The results, taken from eleven experiments all with internal CsCl present to block the large potassium current, are shown in Fig. 10. *B* shows a capacity current record from a demyelinated rabbit

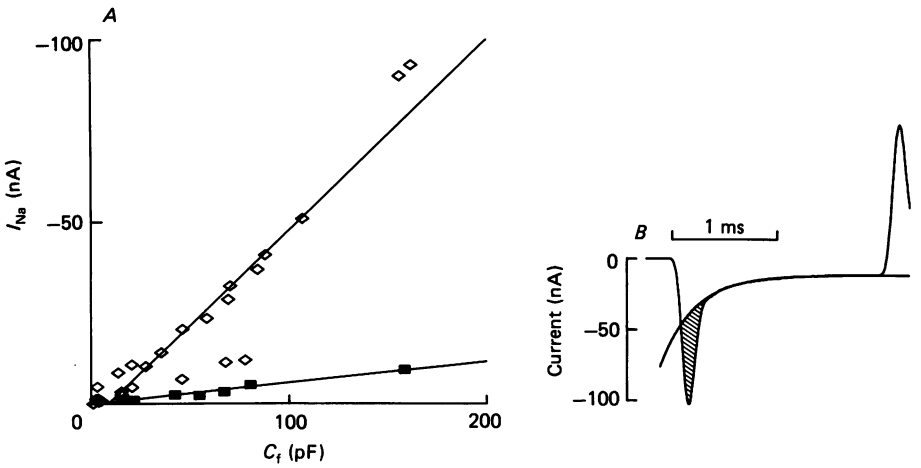

Fig. 10. Comparison of internodal sodium current density in rabbit and frog. *A* shows a plot of fast membrane capacity (C_f) *versus* peak inward sodium current (I_{Na}) in demyelinated internodes from rabbits (open symbols) and frogs (filled symbols). The rabbit internodal currents were from eleven experiments (all with internal CsCl to block potassium currents), and in each experiment the peak values for I_{Na} were measured as C_f increased progressively during demyelination. The frog data was taken from Fig. 10 of Grissmer (1986), and each data point represents the maximum peak current attainable in each experiment. The two straight lines through the points were fitted by a least-squares method with a slope of 0·52 nA/pF (rabbit) and 0·059 nA/pF (frog; Grissmer, 1986). *B* shows the method used to calculate C_f. The capacity and leakage current associated with a hyperpolarizing step from −65 to −115 mV is shown. The smooth curve represents a single exponential function ($\tau = 0{\cdot}3$ ms) fitted to the slow phase of the capacity current. C_f was calculated by using this fitted curve to subtract the slow capacity current from the record, and then dividing the integral of the initial fast capacity current (shaded area) by the size of the hyperpolarizing step. The value of C_f for this record was 162 pF. The capacity current represented the average of four sweeps and was sampled every 10 μs. 2 kHz filter.

internodal segment to illustrate the method used to calculate C_f. The value for C_f was calculated from the charge integral of the initial fast capacity transient (shaded area) by first fitting an exponential function to the slow capacity transient which immediately follows the fast one (see Methods). This method is thus essentially similar to the one adopted by Grissmer (1986) for calculating C_f in the frog internodes. For the record in *B*, $C_f = 162$ pF and the associated sodium current is 93 nA, the highest achieved in this study. From Fig. 10 of Grissmer (1986), the sodium current was only about 9 nA at a similar C_f value. Fig. 10*A* shows a more detailed comparison between the plots of C_f *versus* rabbit (open symbols) and frog (filled symbols) internodal sodium currents. The straight line fitted to all the open symbols (rabbit) has a slope

of 0·52 nA/pF, which is about 9 times larger than the value of 0·059 nA/pF obtained by Grissmer (1986) for frog internodal sodium currents. This comparison suggests that overall internodal sodium current density is significantly higher in the rabbit than in the frog. However, the possibility cannot be excluded that there is a population of rabbit internodes with current density similar to frog (for example, the positions for three open symbols in Fig. 10*A* in the C_f range 50–80 pF are close to the filled symbols).

DISCUSSION

This paper reports for the first time detailed voltage-clamp experiments on acutely demyelinated internodes of mammalian myelinated nerve fibres. As in previous similar studies in the frog internodes (Chiu & Ritchie, 1982; Grissmer, 1986), acute demyelination revealed a large outward potassium current. However, a new finding here of particular interest is the presence of a voltage-gated internodal sodium current. This sodium current is similar to the sodium current that was formerly thought to be restricted to the nodal membranes (Ritchie & Rogart, 1977; Chiu & Ritchie, 1980, 1981). In contrast to the frog, in which an internodal sodium current was either virtually absent (Chiu & Ritchie, 1982) or very small (Grissmer, 1986), the internodal sodium current in the mammal is much larger (by a factor of about 9, Fig. 10*A*) and easily detected. Unlike in frog fibres (Grissmer, 1986), no means could yet be found to maintain an acutely demyelinated internode viable for a prolonged period in mammalian fibres.

The internodal outward current

The large internodal outward current recorded in the rabbit fibres is mostly a potassium current similar to that obtained in frog internodes (Chiu & Ritchie, 1982; Grissmer, 1986). As in the frog internodes, this outward current was much reduced if caesium ions were present in the axoplasm. Figure 9 shows that at a similar degree of demyelination (as measured by the capacity), the outward current was markedly reduced when CsCl, instead of KCl, was present in the axoplasm.

The inhibition by internal caesium ions was incomplete, leaving a small residual outward current. Such an outward current was also seen in the frog internodes (Chiu & Ritchie, 1982; Grissmer, 1986). Grissmer (1986) interpreted this current to be carried by the internal caesium ions slowly penetrating the potassium channel. This small outward current in the rabbit is most likely carried by an inward movement of chloride ions since application of TEA has no effect, and replacement of the external chloride with ascorbate virtually abolished the outward but not the inward tail currents. On the other hand, anions are known to modulate potassium channels; but it could be shown that certain inorganic anions can reduce potassium currents but not organic anions, including ascorbate (Adams & Oxford, 1982).

From Fig. 9, at the same degree of demyelination of 400 pF, the amplitude of the residual current is only about 5% of the total outward current.

The internodal sodium current

The transient inward current is clearly a sodium current similar to that present in excitable membranes; it was inhibited by TTX (Fig. 3), it exhibited a reversal

potential close to the expected Nernstian potential for sodium ions (Fig. 5*A*), and it has voltage-dependent activation and inactivation (Figs 5*A* and 6) with shapes that are similar to those for the sodium channels in the rabbit nodal membrane (see Fig. 12 below).

The recorded currents clearly originated from the internodal segment in the recording pool (pool A, see Fig. 1) and were not artifacts arising from the nodes in the side pools, for the following reasons. First, the nodes in the end pools were surrounded by a CsCl or KCl solution that depolarized the membranes and inactivated the sodium channels. Secondly, the measured reversal potential for the sodium current was about +70 mV, as expected for an external sodium concentration of 150 mM and an internal concentration of 10 mM. Thirdly, voltage-gated chloride currents have not been reported in nodal membranes. Finally, no significant difference in internodal currents was seen in several experiments in which the node in the pool E was cut.

Distortion of voltage-clamp currents by a demyelinated cable

Chiu & Ritchie (1981) have shown, using computer simulations on a cable model with discrete elements, that once a significant degree of demyelination has occurred, the membrane in the recording pool (pool A) is no longer under strict space clamp. An important issue which arises is how reliable are the current records obtained from the most demyelinated fibres in which significant spatial non-uniformities of membrane voltage are expected to develop along the demyelinated membrane. This issue is examined by computer simulations using a cable model similar to that used by Chiu & Ritchie (1981) in previous studies.

Membrane capacitance. An interesting observation in this study is that the total membrane capacity recorded from a highly demyelinated segment could reach a value which greatly exceeds that expected from the axonal membrane in the recording pool alone. For example, the highest total capacity obtained is 600 pF (Fig. 9) which is much higher than the value of about 50 pF expected from only the axonal membrane in the recording pool (length = 100 μm) on the basis of a specific capacitance of 1 μF/cm^2. The first issue to address is whether this surprisingly high value for membrane capacity is an artifact of improper space control in the membrane voltage in the most demyelinated fibres. Fig. 11*D* shows the equivalent circuit used to represent a more or less fully demyelinated internodal segment in the recording pool (pool A). *A* shows an experimental capacity and leakage current record obtained from one of the most demyelinated fibres (same fibre as in Fig. 8*A*). *B* shows the theoretical capacity and leakage current computed using the equivalent circuit on the basis of a specific capacitance of 1 μF/cm^2. The surge of the capacity current in the theoretical current (*B*) is clearly an order of magnitude smaller than that observed (*A*). Thus, the observation of a surprisingly large capacity cannot be explained on the basis of a poorly space-clamped membrane. Indeed, a good fit to the capacity current could be obtained if an unusually high specific membrane capacitance of 10·6 μF/cm^2 is assumed in the calculations (*C*). An interesting implication of this unusually high capacitance (membrane fusion) is discussed in later sections.

Sodium current kinetics. The second issue is whether the sodium currents are so grossly distorted in a fully demyelinated fibre that any resemblance with the nodal sodium currents is purely artifactual. Furthermore, could the extremely large inter-

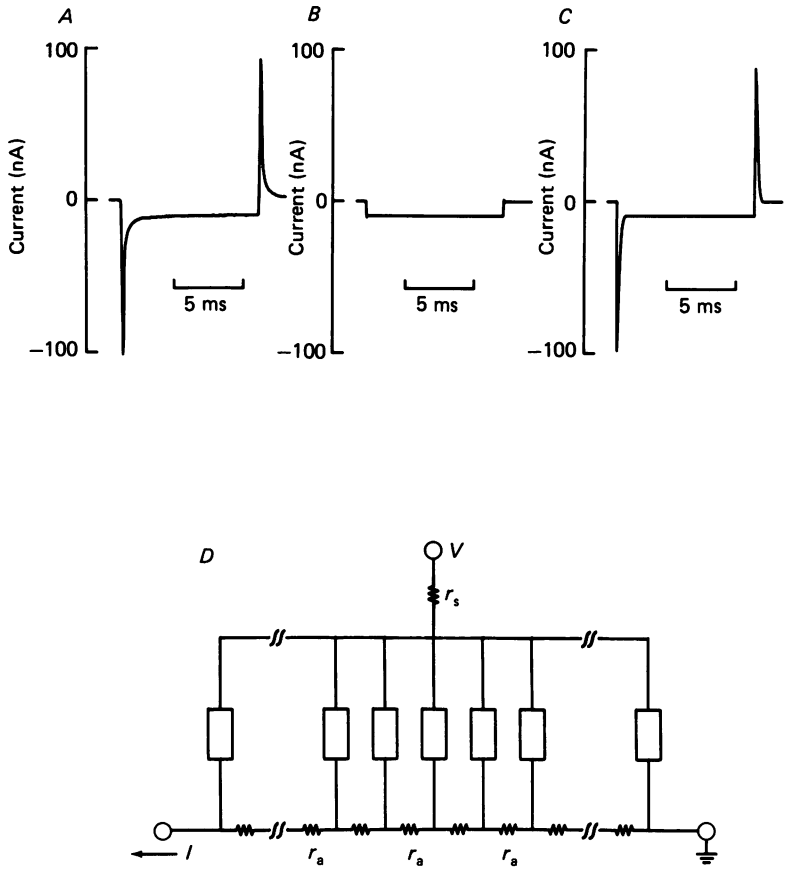

Fig. 11. Computer simulations of the capacity and leakage current in a highly demyelinated internodal segment. *A* shows the observed capacity and leakage current obtained with a hyperpolarizing step of −45 mV in size. The theoretical current in response to the same step change in potential was calculated using the equivalent circuit shown in *D*, with a specific capacitance for the internodal axon of 1 μF/cm^2 (*B*) and 10·6 μF/cm^2 (*C*) respectively. *D* shows the equivalent circuit used for the theoretical computations. The internodal axon (total length of 100 μm) in pool A is represented by ten segments each 10 μm long. The circuit is similar to the one shown in Fig. 10 of Chiu & Ritchie (1981) for computation of paranodal demyelination. Passive membrane properties and sodium conductance are assumed to be homogeneously distributed. Thus each segment has identical values for membrane resistance (R_m), membrane capacity (C_m) and sodium conductance (g_{Na}). r_a represents the longitudinal axoplasmic resistances between adjacent segments and a value of $r_a = 0{\cdot}1$ MΩ is used (see Fig. 10 of Chiu & Ritchie, 1981). r_s represents the series resistance between the recording electrode and the internodal axon. Note that no capacitors were placed between the recording electrode and the internodal axon since the circuit is intended to simulate the condition of more or less full demyelination in which no intact myelin membrane remains. The passive membrane parameters were chosen as follows. First, $(r_s + R_m)$ was chosen to match the steady leakage current. The ratio (r_s/R_m) was then chosen to match the shape of the decline of the capacity current. The specific capacitance of the internodal axon was then adjusted in *C* to match the size of the observed capacity current in *A*; the values used are $r_s = 0{\cdot}45$ MΩ and for each segment, $R_m = 44$ MΩ and $C_m = 50$ pF. For an axonal diameter of 15 μm, this capacity corresponds with a specific capacitance of 10·6 μF/cm^2. *B* was calculated by changing only the specific capacitance from 10·6 to 1 μF/cm^2. (Further details on the method of computation could be found in Figs 10, 11 and 12 of Chiu & Ritchie (1981).)

nodal sodium current observed in the most demyelinated fibres (about 90 nA, Fig. 8*A*) be a greatly overestimation of the actual current because of poor space clamp? These issues are addressed in Fig. 12. Here, *A* shows a family of experimental internodal sodium currents exhibiting the largest amplitude (about 90 nA). The associated capacity current for this family of sodium currents, shown in Fig. 11*A*, has already been used to allow a selection of the appropriate passive membrane properties for the equivalent circuit, as shown in Fig. 11*C*. What would the resultant internodal currents look like if sodium channels with nodal kinetics (Chiu *et al.* 1979) are incorporated into the equivalent circuit of Fig. 11*D*? The result of such a theoretical calculation is shown in Fig. 12*B*. A uniform distribution of sodium conductance at 0·238 μS per 10 μm of internodal length has been chosen to match the amplitudes of the observed currents (*A*). A comparison between *A* and *B* suggests that internodal sodium channels are quite similar to those present in the rabbit node. The family of theoretical currents in *C* is calculated with the same sodium conductance as in *B*, but for the condition of ideal voltage control in which there were no spatial non-uniformities in the membrane voltage (see legend in Fig. 12). The sodium currents in *C* have larger amplitudes when compared to those calculated under conditions in which strict space clamp is not achieved (*B*). Thus, poor space clamp in a highly demyelinated fibre tends to underestimate, rather than overestimate, the actual current density.

Figure 12*E* examines in more detail the distortion of the current–voltage relations for sodium currents due to improper voltage control. By comparing the theoretical curves in which ideal voltage control is achieved (dotted curve) and in which space clamp is not achieved (continuous curve), one can see that an effect of poor space clamp produced by high demyelination is to shift the peak of the current–voltage relation by about 13 mV in the hyperpolarizing direction, from about −37 mV (ideal case, dotted curve) to −50 mV (continuous curve). Interestingly, no significant shift in the theoretical h_∞ curves were produced as a result of poor space clamp during a more or less full demyelination (Fig. 12*F*, compare continuous and dotted curves). A comparison of the actual internodal current data (filled symbols in both *E* and *F*) with the corresponding continuous curves suggests that both the voltage dependence of activation and inactivation of internodal sodium channels are shifted in the depolarizing direction by about 15–20 mV when compared with those from rabbit nodal membrane.

An interesting observation on the inactivation of the internodal sodium channels is that the potential for half-maximal inactivation shifted by 30 mV as demyelination proceeded (Fig. 6). The theoretical calculations in Fig. 12*F* strongly suggest that this shift is unlikely due to a poor voltage clamp since under full demyelination a shift of no more than 2 mV is expected (continuous and dotted curves). One explanation for the shift is that lysolecithin, by virtue of its detergent-like properties, penetrated the membrane and modified the properties of the channels. Indeed, in frog nodes, brief application of lysolecithin was found to shift the nodal h_∞ curve by about 10 mV in the depolarizing direction (S. Y. Chiu, unpublished observations). Another interesting possibility is that the shift reflects a transient trauma to the sodium channels shortly after having been disrupted from the Schwann cell membrane and incorporated into the axonal membrane, as discussed in the later section on membrane fusion.

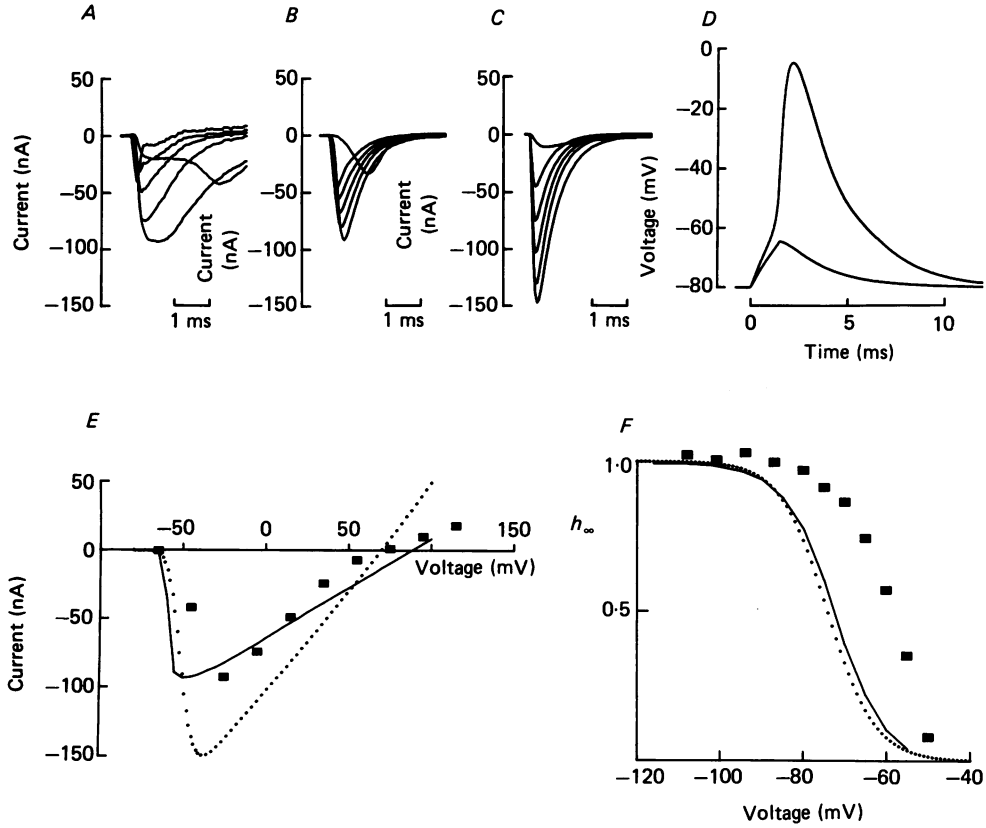

Fig. 12. Theoretical computations of sodium currents and action potential in a demyelinated rabbit internodal segment. The equivalent circuit in Fig. 11 *D* was used to represent a more or less fully demyelinated internodal segment. The passive membrane porperties have been chosen as described in Fig. 11 to match the degree of demyelination as inferred from the experimental capacity current; the corresponding experimental sodium currents from the same experiment are thus used in this Figure for comparison with the theoretical sodium currents. All computations involving sodium currents were based on the set of kinetic equations obtained for the sodium currents in the rabbit nodal membrane (Chiu *et al.* 1979) scaled to 20 °C of the present study (Q_{10} values from Chiu, Mrose & Ritchie, 1979). *A* shows the experimental internodal sodium currents from Fig. 8*C* in which the capacity (degree of demyelination) achieved was the highest in this study. *B* shows the theoretical internodal sodium currents calculated on the assumption that sodium channels are uniformly distributed at a density of $g_{Na} = 0{\cdot}238$ μS per 10 μm of internodal length. *C* shows, for the same g_{Na} value, the currents expected in the ideal case if there were no spatial non-uniformities in the membrane voltage along the demyelinated internodal axon ($r_a = 0$), and that the series resistance (r_s) was zero. The depolarizations are from −45 to +55 mV in 20 mV increments in *A*, and from −60 to +40 mV in 20 mV increments in *B* and *C*. *D* shows a theoretical internodal action potential and a subthreshold response computed with a current stimulus duration of 1·5 ms and the g_{Na} value of *B*. Voltage-dependent potassium conductance was assumed to be zero. The resting potential was assumed to be −80 mV, as in previous calculation for the rabbit nodal action potential (Chiu *et al.* 1979). *E* shows the corresponding current–voltage relations for: *A*, filled symbols; *B*, continuous curve; and *C*, dotted curve. *F* shows how the theoretical h_∞ curves are distorted by demyelination. The theoretical h_∞ curves are calculated by computing the variation in the peak theoretical sodium current

Internodal versus nodal sodium current density in rabbit

How does the density of the internodal sodium channel compare with that from a rabbit node? The following calculations are made without making any specific assumptions as to whether the internodal sodium channels originated from Schwann cells or the internodal axolemma. Under the assumption that the maximal sodium current that can be revealed from a 100 μm segment of internode under optimal conditions of full demyelination is about 90 nA (Fig. 8*C*), the corresponding internodal current density per unit fibre length is 0·9 nA/μm. The peak sodium current elicited from a single rabbit node is about 30 nA at around 19 °C (Table 2 of Chiu, 1980). Thus, assuming that a node is 1 μm wide, the density per unit length for the node is 30 nA/μm, which is about 30 times higher than that of the internodal sodium channels.

Internodal action potential. Even though the internodal sodium current density is low compared to a node, the peak internodal current could exceed the size of the internodal leakage current (Fig. 8*A*), suggesting that it might be possible for an internodal action potential to be generated. Indeed, using the equivalent circuit in Fig. 11*D*, and using the value of the sodium conductance chosen to match the observed peak sodium current (as in Fig. 12*A* and *B*), an internodal action potential could indeed be generated if all potassium channels are blocked (Fig. 12*D*). Thus, the possibility cannot be ruled out that enough sodium channels might normally be present in the internode to support conduction if favourable conditions (like a blockage of the internodal potassium channels) are imposed. This would support the observation of continuous conduction in demyelinated nerve fibres of rat treated with diphtheria toxin (Bostock & Sears, 1978).

Saxitoxin (STX). Even though the internodal sodium current density is only 0·9 nA/μm, the total sodium current of an entire internode of length 1000 μm would be on the order of 900 nA, about 30 times larger than the peak sodium current of 30 nA obtained from a single node. Assuming that the single-channel conductance and kinetics of the internodal sodium channels are similar to nodal sodium channels, that internodal channels are uniformly distributed and that channel density is independent of fibre size, this calculation implies that an entire internode contains 30-fold more sodium channels than a single node in rabbit. Interestingly, Ritchie & Rogart (1977) found that the uptake of labelled STX to rabbit sciatic nerves remained virtually unchanged when the nerves were homogenized. Since homogenization presumably disrupted the Schwann cell and exposed the internodal axon underneath the myelin, a 30-fold increase in STX uptake should have been observed if sodium channels were indeed normally present either on the internodal axolemma under the myelin, or within the Schwann cell membrane foldings. One explanation

---

at a fixed test pulse (to 0 mV) as the potentials of the pre-pulse (20 ms duration) are varied. The dotted curve represents the theoretical h_∞ curve under conditions of perfect voltage control as described in *C*, while the continuous curve shows the theoretical h_∞ curve expected after full demyelination. The filled symbols are the experiment h_∞ relations obtained from an internodal segment with a presumed high degree of demyelination (from Fig. 6). All theoretical computations in Figs 11 and 12 were obtained by numerical integration in steps of 0·2 μs, as described in Chiu & Ritchie (1981).

is that STX sites, though normally hidden within an intact internode, could also be slowly accessible to STX molecules during prolonged incubation periods. If this explanation is correct, only about 1/30 of the observed STX uptake in intact rabbit sciatic nerves is to the node. This would revise the number of STX binding sites per rabbit node from 700000 (Ritchie & Rogart, 1977) down to about 24000. This appears to be well within the upper limit of 83000 sodium channels per rabbit node inferred indirectly from gating current measurements (Chiu, 1980), and clearly close to the value of 21000 sodium channels per node in the rat myelinated nerves determined more directly from noise analysis (Neumcke & Stampfli, 1982).

Origin of the internodal sodium channels

Did lysolecithin uncover pre-existing channels located on the internodal axolemma, or induce incorporation of channels from the Schwann cell to the axon during the process of demyelination ? Even though Chiu & Ritchie (1982) invoked the former suggestion to account for the internodal currents in the frog internodes, it is now clear that the second possibility is also equally plausible.

Recent patch-clamp analysis on a variety of mammalian Schwann cells (Chiu *et al.* 1984; Shrager *et al.* 1985; Chiu, 1987) and astrocytes (Bevan *et al.* 1985) have revealed that they possess voltage-gated sodium, potassium and chloride channels very similar to those detected here in the rabbit internodes. Since lysolecithin is known to induce fusion of biological membranes (Poole *et al.* 1970), membrane fusion between the Schwann cell and the internodal axon could occur in response to this agent. Such a membrane fusion could account for the large capacitance observed at high degrees of demyelination (e.g. 600 pF, Fig. 9). Indeed, the computer simulations in Fig. 11 *B* and *C* show that an unusually high specific capacitance for the internodal axon of 10·6 μF/cm^2 (*C*), rather than the usual 1 μF/cm^2 (*B*), are needed to fit the observed capacity (*A*). Such a high value for the specific capacitance might be expected if extra-axonal membranes (like Schwann cell membrane) are fused with the axonal membrane. On the other hand, a large capacitance exceeding the expected value might also arise from a partially destroyed myelin membrane complex that will have to be charged in addition to the axolemma. However, in the absence of membrane fusion, any Schwann cell membranes in series with the axolemma would tend only to reduce, rather than increase, the total internodal capacitance (see Fig. 11 *D*). If the suggestion of membrane fusion is correct, sodium channels in a Schwann cell could be located on the innermost myelin laminae adjacent to the axon, a highly strategic location for transfer to axons (Shrager *et al.* 1985). Interestingly, recent patch-clamp studies have also raised the possibility that sodium channels on a Schwann cell could be concealed by myelination; sodium currents, which appear on undifferentiated Schwann cells lacking myelin, become virtually undetectable once compact myelin is formed (Chiu, 1987).

The possibility that a Schwann cell can incorporate its own excitable channels onto an axon it ensheaths is a significant one (Shrager *et al.* 1985). It raises an exciting possibility for functional recovery in axons after a demyelinating lesion. Membrane fusion could be one possible mechanism of channel transfer. The results of this study are suggestive, but far from conclusive, that membrane fusion between Schwann cells and axons could occur under special conditions.

We thank Drs H. Meves and B. Neumcke for useful comments on the manuscript, and we acknowledge the assistance of P. Luther and the help with preparing the Figures by Heike Keim. This work was supported in part by the following grants to S. Y. Chiu: NS-23375 from the U.S.P.H.S., RG-1839 from the U.S. National Multiple Sclerosis Society, and a General Research Support Grant to the University of Wisconsin Medical School from the NIH, Division of Research Facilities and Resources.

REFERENCES

ADAMS, D. J. & OXFORD, G. S. (1983). Interaction of internal anions with potassium channels of the squid giant axon. *Journal of General Physiology* **82**, 429–448.

BEVAN, S., CHIU, S. Y., GRAY, P. T. A. & RITCHIE, J. M. (1985). The presence of voltage-gated sodium, potassium and chloride channels in rat cultured astrocytes. *Proceedings of the Royal Society* B **225**, 299–313.

BOSTOCK, H. & SEARS, T. A. (1978). The internodal axon membrane: Electrical excitability and continuous conduction in segmental demyelination. *Journal of Physiology* **280**, 273–301.

CHIU, S. Y. (1980). Asymmetry currents in the mammalian myelinated nerve. *Journal of Physiology* **309**, 499–519.

CHIU, S. Y. (1987). Sodium currents in axon-associated Schwann cells from adult rabbits. *Journal of Physiology* **386**, 181–203.

CHIU, S. Y., MROSE, H. E. & RITCHIE, J. M. (1979). Anomalous temperature dependence of the sodium conductance in rabbit nerve compared with frog nerve. *Nature* **279**, 327–328.

CHIU, S. Y. & RITCHIE, J. M. (1980). Potassium channels in nodal and internodal axonal membrane of mammalian myelinated fibres. *Nature* **284**, 170–171.

CHIU, S. Y. & RITCHIE, J. M. (1981). Evidence for the presence of potassium channels in the paranodal region of acutely demyelinated mammalian single nerve fibres. *Journal of Physiology* **313**, 415–437.

CHIU, S. Y. & RITCHIE, J. M. (1982). Evidence for the presence of potassium channels in the internode of frog myelinated fibres. *Journal of Physiology* **322**, 485–501.

CHIU, S. Y., RITCHIE, J. M., ROGART, R. B. & STAGG, D. (1979). A quantitative description of membrane currents in rabbit myelinated nerve. *Journal of Physiology* **292**, 149–161.

CHIU, S. Y. & SCHWARZ, W. (1987). Are glial Na channels in myelinated fibers strategically located for glia-to-axon transfer? *Biophysical Journal* (in the Press).

CHIU, S. Y., SHRAGER, P. & RITCHIE, J. M. (1984). Neuronal-type Na^+ and K^+ channels in rabbit cultured Schwann cells. *Nature* **311**, 156–157.

GRISSMER, S. (1986). Properties of potassium and sodium channels in frog internode. *Journal of Physiology* **381**, 119–134.

HALL, S. M. & GREGSON, N. A. (1971). The *in vivo* and ultrastructural effects of injection of lysophosphatidyl choline into myelinated peripheral nerve fibres of the adult mouse. *Journal of Cell Science* **9**, 769–789.

NEUMCKE, B. & STAMPFLI, R. (1982). Sodium currents and sodium-current fluctuations in rat myelinated nerve fibres. *Journal of Physiology* **329**, 163–184.

NONNER, W. (1969). A new voltage clamp method for Ranvier nodes. *Pflügers Archiv* **309**, 176–192.

POOLE, A. R., HOWELL, H. I. & LUCY, J. A. (1970). Lysolecithin and cell fusion. *Nature* **227**, 810–813.

RITCHIE, J. M. & ROGART, R. B. (1977). The density of sodium channels in mammalian myelinated nerve fibers and the nature of the axonal membrane under the myelin sheath. *Proceedings of the National Academy of Sciences of the U.S.A.* **74**, 211–215.

SHRAGER, P., CHIU, S. Y. & RITCHIE, J. M. (1985). Voltage-dependent sodium and potassium channels in mammalian cultured Schwann cells. *Proceedings of the National Academy of Sciences of the U.S.A.* **82**, 948–952.

SIGWORTH, F. J. (1980). The variance of sodium current fluctuations at the node of Ranvier. *Journal of Physiology* **307**, 97–129.

WAXMAN, S. G. & RITCHIE, J. M. (1985). Organization of ion channels in the myelinated nerve fiber. *Science* **228**, 1502–1507.

WEBSTER, G. R. & ALPERN, R. J. (1964). Studies on the acylation of lysolecithin by rat brain. *Biochemistry Journal* **90**, 35–42.